Preprint typeset in JHEP style - HYPER VERSION

ISW effect as probe of features in the expansion history of the Universe

Santanu Das

Inter-University Centre for Astronomy and Astrophysics, Post Bag 4, Ganeshkhind, Pune 411 007, India
E-mail: santanud@iucaa.ernet.in

Arman Shafieloo

Asia Pacific Center for Theoretical Physics, Pohang, Gyeongbuk 790-784, Korea
&
Department of Physics, POSTECH, Pohang, Gyeongbuk 790-784, Korea
&
Institute for the Early Universe, Ewha Womans University, Seoul, 120-750, Korea
E-mail: arman@apctp.org

Tarun Souradeep

Inter-University Centre for Astronomy and Astrophysics, Post Bag 4, Ganeshkhind, Pune 411 007, India
E-mail: tarun@iucaa.ernet.in

Abstract: In this paper, using and implementing a new line of sight CMB code, called CMBAns [1], that allow us to modify $H(z)$ for any given feature at any redshift we study the effect of changes in the expansion history of the Universe on the CMB power spectrum. Motivated by the detailed analytical calculations of the effects of the changes in $H(z)$ on ISW plateau and CMB low multipoles, we study two phenomenological parametric form of the expansion history using WMAP data and through MCMC analysis. Our MCMC analysis shows that the standard ΛCDM cosmological model is consistent with the CMB data allowing the expansion history of the Universe vary around this model at different redshifts. However, our analysis also show that a decaying dark energy model proposed in [2] has in fact a marginally better fit than the standard cosmological constant model to CMB data. Concordance of our studies here with the previous analysis showing that Baryon Acoustic Oscillation (BAO) and supernovae data (SN Ia) also prefer mildly this decaying dark energy model to ΛCDM, makes this finding interesting and worth further investigation.

Contents

There are always theoretical degeneracies that makes it hard to distinguish between different cosmological models. Though the standard spatially flat ΛCDM model with power-law form of the primordial spectrum provides a reasonably good fit to all cosmological observations using a handful set of parameters, there is still space for some other models to have a good concordance to the data. Using different cosmological observations to probe a cosmological quantity is one of the best ways we can approach this problem to break the degeneracies between different models. One of the key problems in cosmology is to recover the dynamics of the Universe and reconstruct the expansion history of the Universe and so far supernovae type Ia (SN Ia) as standardised candles and Baryon Acoustic Oscillation (BAO) data as standard rulers have been the two main direct probes of the expansion history. It is also known that changes in the expansion history of the Universe can affect the angular power spectra of the Cosmic Microwave Background particularly at low multipoles through Integrated Sachs Wolf (ISW) effect [3], however little has been done in this direction [4–6] due to complications of the analysis and indirect effect of the expansion history on the CMB observables. In this paper we study the effect of changes in the expansion history of the Universe on the CMB angular power spectrum using a new CMB line of sight code called CMBAns [1] developed and implemented to work on different forms of $H(z)$. The advantage of this approach over using publicly available softwares such as CAMB [7] is that we can work on any desired form of $H(z)$ directly rather than considering different dark energy models with equation of state of dark energy as an input. Considering perturbed or un-perturbed dark energy, working on $H(z)$ would be in fact a generalised study of different dark energy models which may have similar effect on the expansion history of the Universe. After a detailed

analytical calculations of the effects of changes in $H(z)$ on CMB low multipoles, we study two phenomenological models of the expansion history of the Universe where both models include $\omega_{DE} = -1$ model as a possibility through MCMC analysis and using WMAP CMB data [8].

We show that we can in fact use ISW effect to put reasonable constraints on the expansion history of the Universe at distances that are beyond the reach of supernovae or large scale structure data. We also show that while standard ΛCDM model has a good concordance to the data allowing $H(z)$ to vary around this model, a decaying dark energy model proposed in [2, 9, 10] has also a very good fit to the data and in fact marginally better than best fit ΛCDM model which makes this model interesting.

In the following first we go through some analytical calculations and see how changes in the expansion history of the Universe can affect the CMB low multipoles. Then we study two simple phenomenological models of the expansion history where both of these models include ΛCDM as a possibility in order to study how far we can deviate from the standard model and still have a good fit to the data. Then we present results and conclude.

1. Problem formulation

The CMB power spectrum is one of the most precisely measured quantities in the theoretical astrophysics. There is no simple analytical expression for calculating the CMB power spectrum with sufficient accuracy to match the observations and numerical evaluation as carried out here with an independent Boltzman code. An expression for calculating the CMB temperature power spectrum [11, 12] can be written as

$$C_l = \int_0^\infty |\Delta_l(k)|^2 P(k) k^2 dk \ . \tag{1.1}$$

Here, $\Delta_l(k)$ is the brightness fluctuation function and $P(k)$ is the primordial power spectrum. The brightness fluctuation function can be written in terms of the temperature source terms ($S_T(k,\tau)$) and the spherical Bessel function ($j_l(x)$) of order l as

$$\Delta_l(k) = \int_0^{\tau_0} S_T(k,\tau)\, j_l(k(\tau_0 - \tau)) d\tau \ , \tag{1.2}$$

where τ is the conformal time and τ_0 represents the conformal time at the present epoch i.e. at redshift $z = 0$ and k is the wave number. The exact expression for the temperature source term in conformal gauge is given by

$$S_T(k,\tau) = g\left(\delta_g + \Psi - \frac{\dot{\theta}_b}{k^2} - \frac{\Pi}{4} - \frac{3\ddot{\Pi}}{4k^2}\right) + e^{-\mu}\left(\dot{\phi} + \dot{\Psi}\right) - \dot{g}\left(\frac{\theta_b}{k^2} + \frac{3\dot{\Pi}}{4k^2}\right) - \frac{3\ddot{g}\Pi}{4k^2}\ . \tag{1.3}$$

Here μ is the optical thickness at time τ, g is visibility function and is given by $g = \dot{\mu}\exp(-\mu)$, δ_g is the photon density fluctuation i.e. $\delta_g = \delta\rho_g/\rho_g$ where ρ_g is the density of photons, $\theta_b = kv_b$, where v_b represents the velocity perturbation of the baryons, ϕ and Ψ are the metric perturbation variable where the line element is given by $ds^2 = a^2(\tau)\left\{-(1+2\Psi)\,d\tau^2 + (1-2\phi)\,dx^i dx_i\right\}$, and $a(\tau)$is the scale factor. Here i's run from 1 to 3. Π is the anisotropic stress and in most of the cases Π and its derivatives i.e. $\dot{\Pi}$ and $\ddot{\Pi}$ can be neglected because they are small in comparison to the other terms. In all the expressions overdot ($\dot{x}$) denotes the derivative with respect to the conformal time.

The first term in the bracket in Eq.1.3 can be interpreted in terms of the fluctuations in the gravitational potential at the last scattering surface and is referred as the Sachs-Wolfe (SW) term. The second term provides an integral over the perturbation variables along the line of sight to the present era. This can be interpreted in terms of variations in the gravitational potential along the line of sight and this is often referred to as the Integrated Sachs-Wolfe (ISW) term. The third term is known as the Doppler term and is arose from the Doppler effect caused by the velocity perturbation of the photons at the surface of last scattering.

The visibility function g and its derivative $\dot{g}$ only peak at the surface of the last scattering provided there is no re-ionization and in all the other parts it is zero. Therefore, the SW and the Doppler term is only important at the surface of the last scattering. As the ISW part is not multiplied with any such visibility function therefore it is important throughout the expansion history. The ISW part can be broken in two parts, 1) the ISW effect before the surface of last scattering or the early ISW effect and 2) after the surface of last scattering or the late ISW effect. Therefore, the total source term can actually be broken into two independent parts, provided there is no re-ionization,

$$S_T(k,\tau) = S_T^{Pri}(k,\tau) + S_T^{ISW}(k,\tau)\ . \tag{1.4}$$

Here the $S_T^{Pri}(k,\tau)$, i.e. the primordial part consists of the SW, Doppler and the early ISW part. The $S_T^{ISW}(k,\tau)$ part consists of the late time ISW part. As the dark energy only dominates at the late time in the Universe therefore dark energy only affect the ISW source term. The primordial source term will be completely unaffected by the dark energy provided there is no re-ionization.

The quantity we are interested in any CMB experiments is the angular power spectrum, C_l and Eq.1.4 shows that there are three independent terms in C_l,

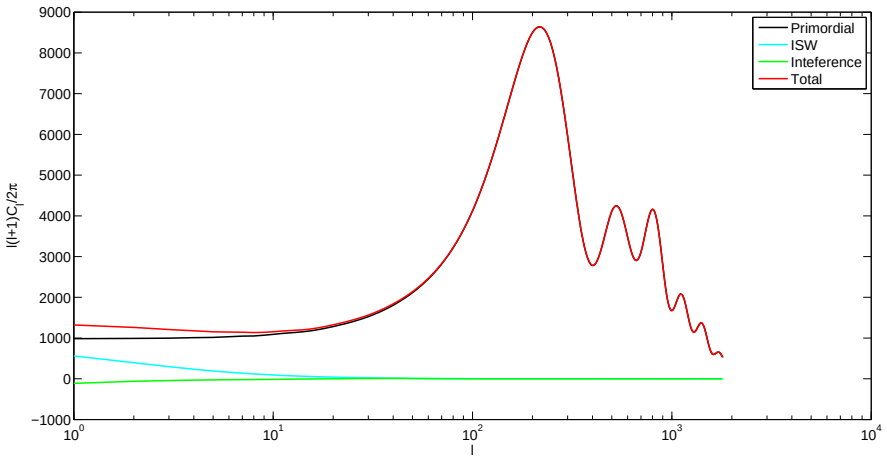

Figure 1: Form of the angular power spectrum for ΛCDM model without the re-ionization and lensing effect. Black line represent the primordial part C_l^{Pri}, cyan line is for the ISW part C_l^{ISW} and the green line shows the interference part C_l^{Int}. Red plot is showing the total angular power spectrum $C_l = C_l^{Pri} + C_l^{ISW} + 2C_l^{Int}$. At low multipoles the power from the primordial part is almost constant. The increase in the power at low multipoles arises from the ISW and the interference part.

$$C_l = C_l^{Pri} + C_l^{ISW} + 2C_l^{Int} \ . \tag{1.5}$$

The first term, which is

$$C_l^{Pri} = \int_0^\infty k^2 dk \left\{ \int_0^{\tau_0} \left[g\left(\delta_g + \Psi - \frac{\dot{\theta}_b}{k^2}\right) - \dot{g}\left(\frac{\theta_b}{k^2}\right) \right] j_l((\tau_0 - \tau)k) d\tau \right. \\ \left. + \int_0^{\tau_*} \left[e^{-\mu}\left(\dot{\phi} + \dot{\Psi}\right) \right] j_l((\tau_0 - \tau)k) d\tau \right\}^2 , \tag{1.6}$$

is the contribution from pure SW, doppler effect and the early ISW. This quantity is always positive since the integrand being a squared term is positive. The second term

$$C_l^{ISW} = \int_0^\infty k^2 dk \left\{ \int_{\tau_*}^{\tau_0} \left[e^{-\mu}\left(\dot{\phi} + \dot{\Psi}\right) \right] j_l((\tau_0 - \tau)k) d\tau \right\}^2 \tag{1.7}$$

is the contribution from the late time ISW part. This part is also positive because of the similar reason. As ISW effect is only important at low multipoles, C_l^{ISW} will provide a positive power at low multipoles. ϕ and Ψ are the perturbed gravitational potential and they directly depend on the expansion history of the Universe, i.e. $H(z)$.

The third term

$$C_l^{Int} = \int \Delta_l^{Pri}(k)\Delta_l^{ISW}(k)P(k)k^2dk \tag{1.8}$$

is the interference term between the primordial and ISW source terms. The term C_l^{Int} is important because unlike the other two terms, C_l^{Int} can either be positive or negative. If we separate out the three terms then it can be seen that for ΛCDM the interference term is actually negative. The interference term in case of the ΛCDM model is very small as the two spherical Bessel functions from the two independent parts are in general out of phase and cancel each other. Therefore, the ISW term as a whole $(C_l^{ISW} + C_l^{Int})$ typically increases the power at the low C_l multipoles.

In Fig.1, all three components of the Sachs-Wolfe effect for the ΛCDM model are shown independently. It can be seen that the primordial part is almost flat at the low multipoles and the increase of power at the low multipole is coming from the ISW part. It is known that in case of the SCDM model the derivative of the potentials are zero after the surface of the last scattering so no late time ISW effect exist there. It is also known that the $H(z)$ varies faster in case of SCDM model then that of standard ΛCDM model. So if we increase the $H(z)$ at the low redshift then it is possible to decrease the power at the low CMB multipole. Increasing the $H(z)$ slightly at the low redshift actually induces two effects. First, it may decrease the power of the C_l^{ISW} term and second it may make the C_l^{Int} part more negative and hence it may decrease the power at the low C_l multipoles.

Here it can be noted that the ISW effect does not change the CMB polarization power spectrum. The source term for the E mode polarization is given by

$$S_E(k,\tau) = \frac{3}{16}\frac{g(\tau)\Pi(k,\tau)}{x^2}\ , \tag{1.9}$$

where $x = k(\tau_0 - \tau)$. As there is no potential dependent term, E mode polarization source term remain unaffected by the ISW effect provided the distance of the last scattering surface from the present era remains fixed. So the polarization power spectrum i.e. C_l^{EE} will remain fixed whereas the cross power spectrum i.e. C_l^{TE} will show some changes at low multipoles.

In this work we have perturbed the Hubble parameter from the standard ΛCDM model and calculated the angular power spectrum. It may be noted that the $H(z)$ has been chosen to match the ΛCDM model at the present redshift and the early epoch and deviating from the ΛCDM model only occurs at some intermediate range. The details of the models are discussed in the next section. Later on in this paper we will also study a particular decaying dark energy model, suggested in [2, 9, 10] where at low redshifts $H(z)$ can have a larger values than $H(z)$ of ΛCDM model that has been suggested by SN Ia and BAO data and show that this model provides consistent fit to the CMB data.

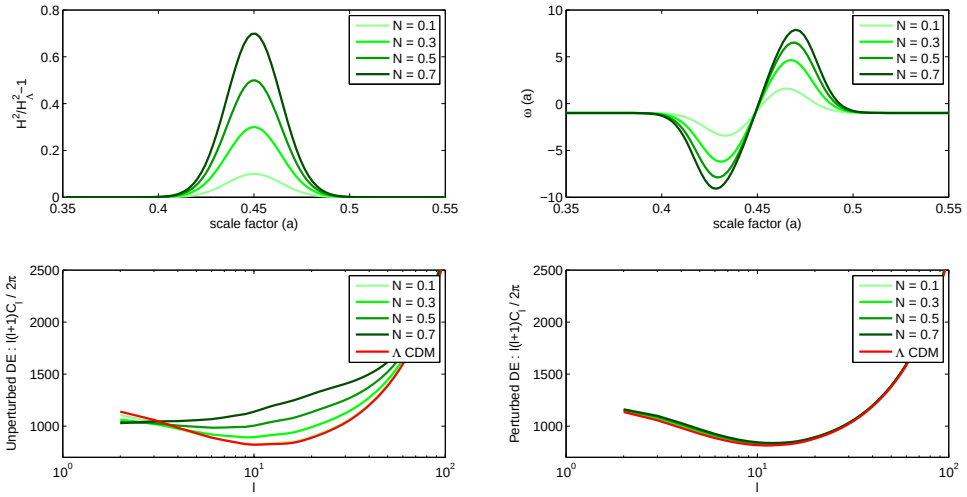

Figure 2: Plots for different N (amplitude of the Gaussian bump) using Eq.2.1 for $H(z)$. The other two parameters are kept fixed at $a_d = 0.45$ and $da = 0.02$. Top-left : Plots of $\frac{H^2}{H_\Lambda^2} - 1$ as a function of scale factor. Top-right : The equation of state of dark energy ($\omega(a)$) as a function of scale factor. Bottom-left : Angular power spectrum for unperturbed dark energy. Bottom-right: Angular power spectrum for perturbed dark energy.

2. Changing the Expansion History

As we have mentioned earlier, we study possible deviations in $H(z)$ from the standard ΛCDM model with respect to the CMB measured angular power spectrum from WMAP. We choose to put a Gaussian deviation from the $H(z)$ expected from the standard ΛCDM model at a particular redshift,

$$\frac{H(z)}{H_\Lambda(z)} = \left\{1 + N \exp\left[-\left(\frac{a - a_d}{da}\right)^2\right]\right\}^{1/2} \tag{2.1}$$

where $H_\Lambda(z)$ is the expansion history expected from ΛCDM model, a_d is the scale factor where we are putting the Gaussian bump, da is the width of the Gaussian bump and N_0 is the amplitude of the Gaussian bump.

There are two different ways to consider this perturbation in the expansion history. Firstly, there can be different models such as extra dimensional models of different scalar field models where the dark energy can only change the expansion history of the Universe and is not perturbed. There can be a second type of dark energy models where the dark energy can itself gets perturbed. In these models not only dark energy affect the background expansion rate, but its perturbation also directly changes the power spectrum. In this paper we have analysed both types of these models.

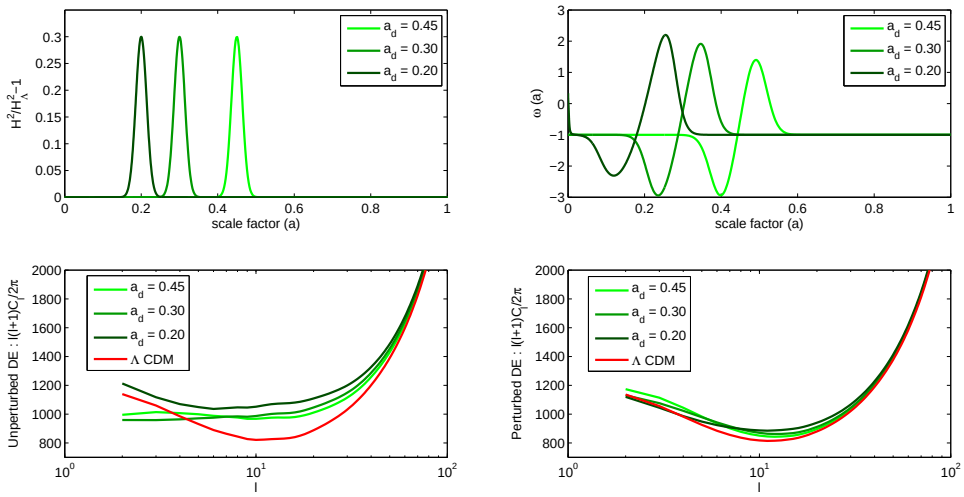

Figure 3: Plots for different a_d (scale factor of the assumed Gaussian bump) using Eq.2.1 for $H(z)$. The other two parameters are kept fixed at $N = 0.3$ and $da = 0.05$. Top-left : Plots of $\frac{H^2}{H_\Lambda^2} - 1$ as a function of scale factor. Top-right : The equation of state of dark energy $(\omega(a))$ as a function of scale factor. Bottom-left : Angular power spectrum for unperturbed dark energy. Bottom-right : Angular power spectrum for perturbed dark energy.

While $H(z)$ is given by Eq.2.1, dark energy equation of state and the $H(z)$ are related by the equation

$$w(a) = 1 - \frac{\frac{2}{3}\frac{a}{H(a)}\frac{dH(a)}{da} - \Omega_{0m}\frac{H_0^2}{H^2(a)}}{1 - \Omega_{0m}\frac{a^3}{H^2(a)}H_0^2} \ . \tag{2.2}$$

Here we have considered that Ω_r is very small at the era we are interested in and therefore the contribution from the radiation part i.e. Ω_r can be neglected. H_0 is the Hubble parameter at the present time and Ω_{0m} is the matter density, i.e. $\Omega_{0b}+\Omega_{0CDM}$ (also at the present era). In our case the expansion history can be written as

$$\frac{H^2(a)}{H_0^2} = \left(\frac{\Omega_{0m}}{a^3} + \Omega_\Lambda\right)\left(1 + N\exp\left(-\left(\frac{a-a_d}{da}\right)^2\right)\right) \ , \tag{2.3}$$

and after few simple algebraic manipulation one can show that

$$\frac{1}{H^2(a)}\frac{dH^2(a)}{da} = -\left[\frac{\frac{3\Omega_{0m}}{a^2}}{\frac{\Omega_{0m}}{a^3} + \Omega_\Lambda} + \left(\frac{2}{da}\right)\left(\frac{a-a_d}{da}\right)\frac{N\exp\left(-\left(\frac{a-a_d}{da}\right)^2\right)}{1 + N\exp\left(-\left(\frac{a-a_d}{da}\right)^2\right)}\right] \ . \tag{2.4}$$

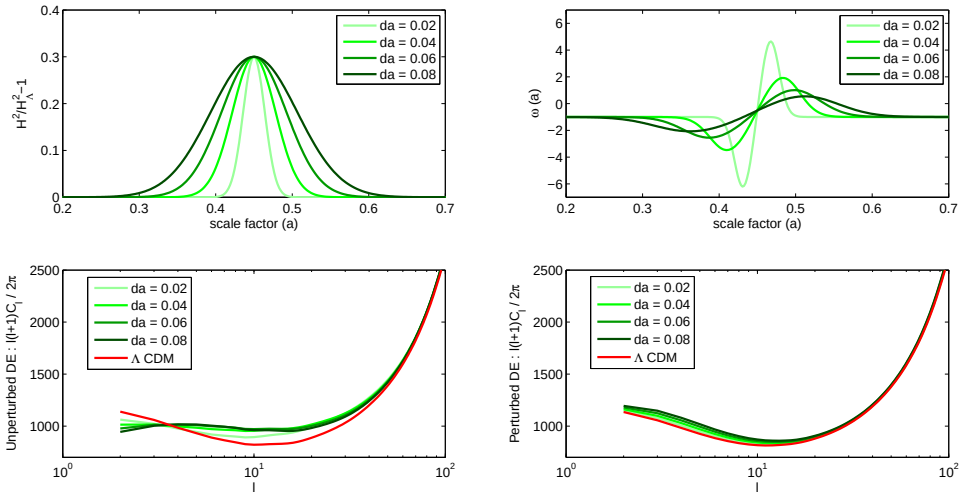

Figure 4: Plots for different da (width of the Gaussian bump) using Eq.2.1 for $H(z)$. The other two parameters are kept fixed at $a_d = 0.45$ and $N = 0.3$. Top-left : Plots of $\frac{H^2}{H_\Lambda^2} - 1$ as a function of scale factor. Top-right : The equation of state of dark energy ($\omega(a)$) as a function of scale factor. Bottom-left : Angular power spectrum for unperturbed dark energy. Bottom-right : Angular power spectrum for perturbed dark energy.

Using Eq.2.2, Eq.2.3 and Eq.2.4 we can find out $\omega(a)$ as a function of the scale factor. The perturbation equation which we have used for the dark energy [13, 14]are given by

$$\dot{\delta}_x = -3H\left(c_s^2 - \omega_x\right)\left(\delta_x + 3H\left(1+\omega_x\right)\frac{\theta_x}{k^2}\right) - \left(1+\omega_x\right)\theta_x - 3\left(1+\omega_x\right)\dot{h} \qquad (2.5)$$

and

$$\frac{\dot{\theta}_x}{k^2} = -H\left(1 - 3c_s^2\right)\frac{\theta_x}{k^2} + \Psi + c_s^2\delta_x/\left(1+\omega_x\right) \ . \qquad (2.6)$$

Here $c_s^2 = \frac{\delta P_x}{\delta \rho_x}$ and c_s^2 is kept to be unity in the analysis. δ_x is the density perturbation of the dark energy and $\theta_x = ku_x$, where k is the wave number and u_x is the velocity perturbation of the dark energy. $\dot{h} = \left(\frac{\dot{\delta a}}{a}\right)$ where the over-dot denotes the derivative with respect to the conformal time.

In Fig.2 we show the computed power spectrum for different N values but constant a_d and da cases. Fig.3 shows the plots for variable a_d and the Fig.4 shows plots for variable da. Except the bump parameters all other parameters for the model are same as that of the standard ΛCDM model. Plots are made for both perturbed and unperturbed dark energy models and the plot for the standard ΛCDM is also shown for comparison. One can notice that the unperturbed dark energy has more effect

on the low CMB multipoles through ISW effect (in comparison with perturbed dark energy).

3. Results and Discussion

3.1 Bump Model

The parametric form of $H(z)$ we use in this analysis given by Eq.2.1 allows us to study how far we can deviate from the standard ΛCDM model at different redshifts while still keeping the concordance to the CMB data. This parametric form can also give us a hint if a particular smooth deviation from the expansion history given by the standard model may rise to a better fit to the CMB data and hence can be used to test the consistency of the standard ΛCDM model to the CMB observations.

In this analysis, we have used a numerical package called CMBAns [1]. For unperturbed dark energy models the $H(z)$ has been changed directly and its effects are analysed. In the case of perturbed dark energy, along with the modification of the $H(z)$, the dark energy velocity and density perturbations are included with the other perturbation equations. These dark energy perturbations change the potential at the late time and hence also influence the ISW effect.

For finding out the best fit set of parameters, a MCMC code using the global metropolis algorithm has been used. The MCMC code uses CMBAns [1] for calculating the theoretical power spectra (temperature and polarization) and the WMAP likelihood [17] code for calculating the likelihood of the theoretical power spectrum using the WMAP 7 year data [8]. We have chosen a flat prior for all cosmological parameters.

Four set of analysis have been carried out with the Gaussian deviation in the $H(z)$. The first set uses a 9 parameter set amongst which 6 are the standard cosmological parameters, namely baryon density $\Omega_b h^2$, total matter density $\Omega_{0m} h^2$, H_0, the Hubble parameter in a units of $100\,km/s/Mpc$, re-ionization optical depth (τ), scalar spectral index (n_s) and the primordial primordial power spectrum amplitude (A_s). Apart from these 6 standard parameters we have used three extra parameters for modifying the $H(z)$ using a Gaussian bump. These are the amplitude of the Gaussian bump N, the red shift or scale factor a_d at which the Gaussian bump is placed and the width/standard deviation of the Gaussian bump da. In Fig.5a we have shown the two dimensional likelihood of the parameters from the MCMC analysis. The plots shows that Gaussian parameters are almost uncorrelated with all the cosmological parameters except the H_0 (h) and A_s. There is a mild negative correlation between h and N with correlation coefficient 0.32. As the Gaussian bump parameters are very much uncorrelated with the standard model parameters therefore we can expect all the parameters to be very much close to the standard model parameters. The one dimensional marginalized probability distribution for

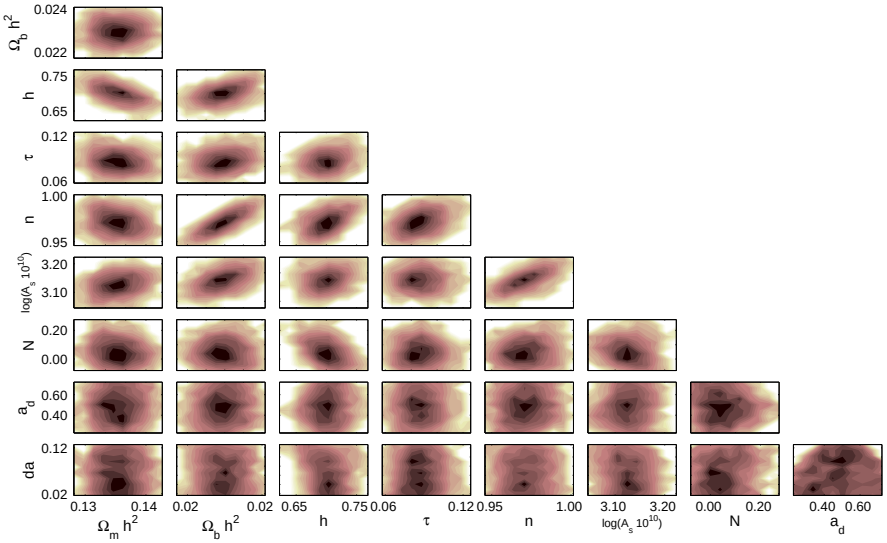

(a) Two dimensional likelihood contours for the set of 9 cosmological parameters

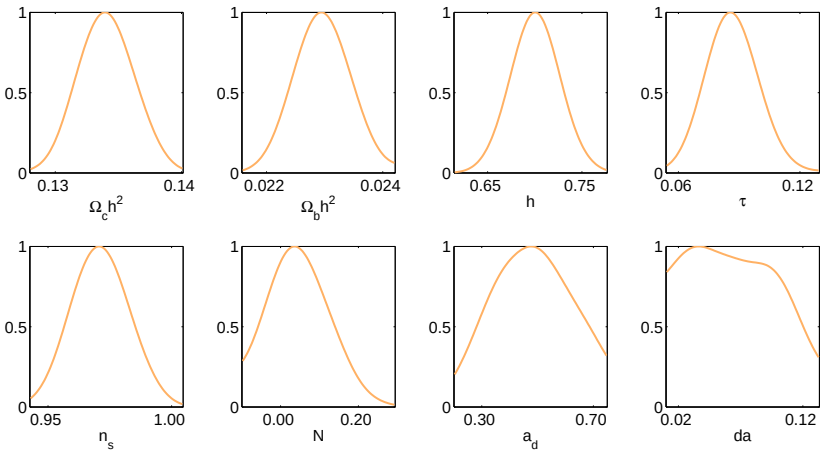

(b) One dimensional marginalized probability distribution

Figure 5: Cosmological parameter estimation (9 parameters) assuming no perturbation for dark energy. $H(z)$ for the model is given by Eq.2.1.

the 8 parameters are shown in Fig.5b. It shows that the distribution for *da* is almost flat for a wide range of values. Therefore the convergence of the Gelman Rubin statistics for *da* is very slow. The average values of the parameters and their standard deviation are given in the table 1. The results shows that the expansion rate of the Universe can deviate up to 20% from the $H(z)$ given by ΛCDM model at some redshifts however, the data seems to be clearly consistent with the ΛCDM model and in fact adding these features to $H(z)$ seems not to significantly impact the fit to the data. Another noticeable result is that h is allowed to have a smaller values

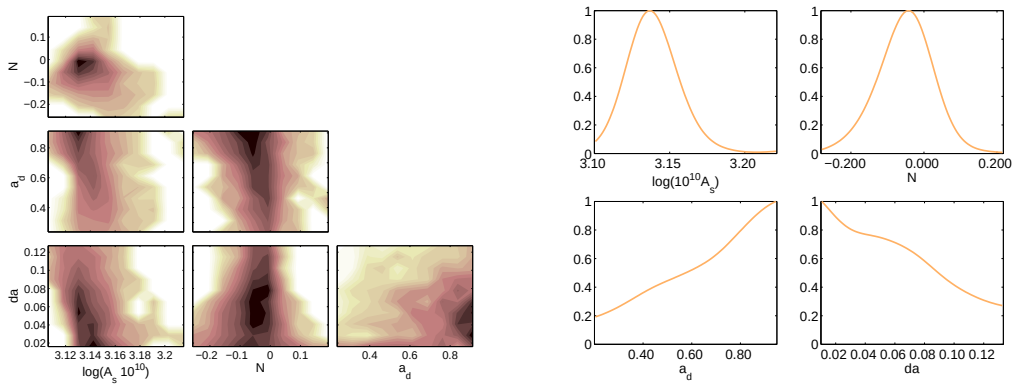

(a) Two dimensional likelihood contours for the set of 4 parameters

(b) One dimensional marginalized probability distribution

Figure 6: Parameter estimation for the bump model assuming no perturbation for dark energy. $H(z)$ for the model is given by Eq.2.1 and other cosmological parameters are fixed at their best fit ΛCDM values.

than those expected from the ΛCDM model.

The second analysis is carried out with a 4 parameter set. In this case we keep all the standard cosmological parameters, except A_s, fixed at their best fit ΛCDM model values. The parameters which we use as the free parameters here are the parameters of the Gaussian bump, i.e. N, a_d and da. As A_s scales the power spectrum, it is important to make it a free parameter. Results are shown in Fig.6. In Fig.6a we have plotted the two dimensional likelihood contours for the set of 4 parameters. The plots are showing that none of the two parameters are correlated. In Fig.6b the one dimensional marginalized probability distributions are plotted. The plots are showing that when we fix all the other cosmological parameters (to the values given by standard model), the constraints on the bump parameters become tighter. However, height of the Gaussian bump indicates that still we can have up to 20% deviation from $H(z)$ given by ΛCDM at some intermediate redshifts. The width of the Gaussian bump also becomes narrower not allowing to deviate from ΛCDM model continuously in a broad range. This is something expected as we have fixed all the other parameters in the analysis so the constraints on the remaining ones must become statistically tighter. The average value of the fitted parameter are tabulated in table 1.

The third analysis is carried out with 9 parameters but with the perturbed dark energy model. The parameter set is same as that of the first parameter set. The results are shown here in Fig.7. The two dimensional likelihood plots are shown in Fig.7a and the one dimensional marginalized probability distribution for the 8 parameters are shown in Fig.7b. Here also we can see that there are some correlation between the bump parameter and the Hubble parameter. Apart from that the bump

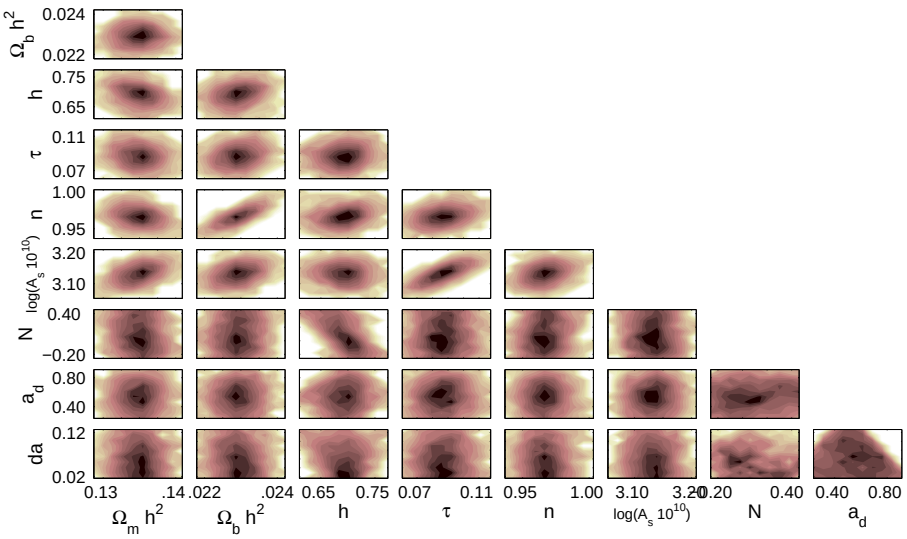

(a) Two dimensional likelihood contours for the set of 9 cosmological parameters

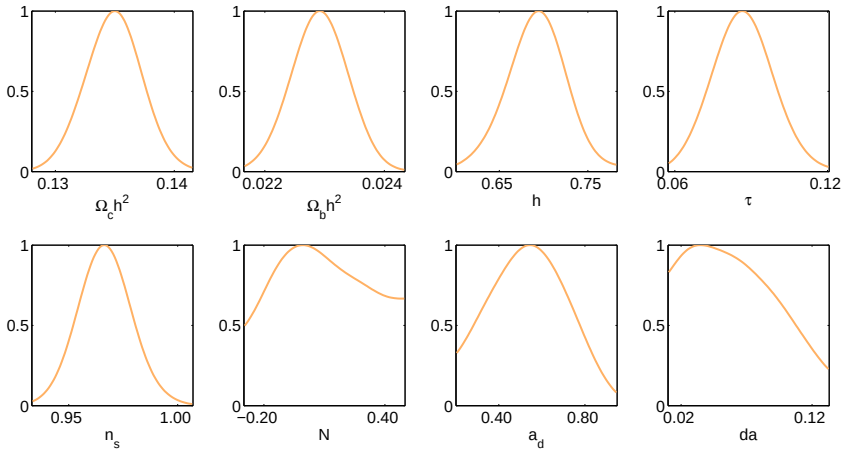

(b) One dimensional marginalized probability distribution

Figure 7: Cosmological parameter estimation (9 parameters) assuming perturbed dark energy. $H(z)$ for the model is given by Eq.2.1.

parameters are very much uncorrelated with all the other cosmological parameters. Here also it can be seen that the distribution of N and da are much flatter near the peak. This can also be seen from the standard deviations. The standard deviation for N is much larger in this case in comparison to the previous unperturbed DE case. This allows up to 40% deviation from the expansion history given by ΛCDM model at some intermediate redshifts around $z \approx 0.6$. The average value of the fitted parameter are tabulated in table 1 .

In the fourth we have analysed the perturbed dark energy model with a 4 parameter set. All the standard cosmological parameters expect A_s are kept fixed.

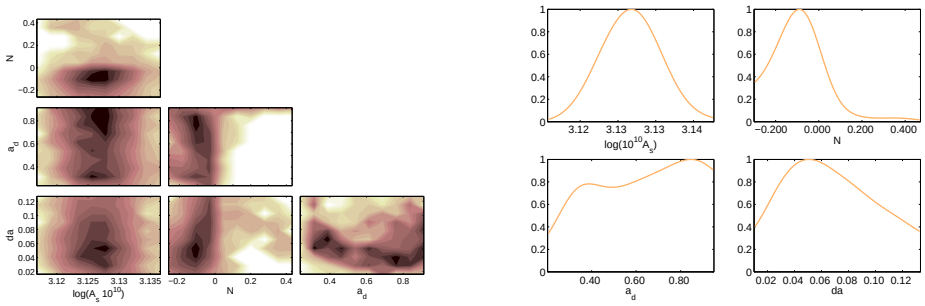

(a) Two dimensional likelihood contours for the set of 4 parameters

(b) One dimensional marginalized probability distribution

Figure 8: Parameter estimation for the bump model assuming perturbation for dark energy. $H(z)$ for the model is given by Eq.2.1 and other cosmological parameters are fixed at their best fit ΛCDM values.

The two dimensional likelihood plots are shown in Fig.8a and the one dimensional marginalized probability distribution for the parameters are shown in Fig.8b. The plots show that a_d is following some double humped kind of distribution and the average likelihood is quite independent of the Gaussian parameters. The average value of the fitted parameter are tabulated in table 1. These results show that while we can in fact deviate significantly from the expansion history of the universe given by the standard ΛCDM model at some intermediate redshifts and still having a good fit to the data, but having the standard model close to centre of confidence contours indicates toward robust consistency of the standard model to the data. Getting only mild improvement in the likelihood to the data assuming few more degrees of freedom, hints towards the fact that any Bayesian analysis would still favour ΛCDM to the alternative ones.

3.2 Decaying Dark Energy Model

Another set of analysis have been carried out using a parametric form of the dark energy equation of state that allows the expansion of the Universe undergo a slowing down in its acceleration at low redshifts. The particular equation of state has been analysed by Shafieloo et.al. in [2, 9, 10] to show that slowing down of the acceleration in the expansion history of the Universe which might come from a decaying dark energy model, can in fact improve the fit to both supernovae and BAO data.

The dark energy equation of state is here taken as

$$\omega(z) = -\left[1 + \tanh((z - z_t)\Delta z)\right]/2. \tag{3.1}$$

This simple parametric form allows equation of state of dark energy to change rapidly at low redshifts while at higher redshifts it behaves exactly similar to ΛCDM

	Unperturbed (9 par)	Unperturbed (4 par)	Perturbed (9 par)	Perturbed (4 par)
$\Omega_b h^2$	0.0224± 0.0004	0.0224	0.0224±0.0004	0.0224
$\Omega_{0m} h^2$	0.1332±0.0038	0.1336	0.1348±0.0040	0.1336
h	0.6997±0.0201	0.705	0.6897±0.0268	0.705
τ	0.0865±0.0108	0.0848	0.0869±0.0103	0.0848
n_s	0.9708±0.0114	0.968	0.9670±0.0099	0.968
$\log(10^{10} A_s)$	3.1254±0.0281	3.1421±0.0041	3.1319±0.0251	3.1252±0.0014
N	0.0478±0.0624	-0.0523±0.0225	0.1215±0.2030	-0.1085±0.0296
a_d	0.4798±0.1297	0.5938±0.0745	0.5938±0.0745	0.5389±0.0724
da	0.0617±0.0316	0.0505±0.018	0.0594±0.0298	0.0606±0.0116
$\Delta\chi^2$	0.3	0.2	1.4	0.7

Table 1: Estimated cosmological parameters for the bump model. $H(z)$ for the model is given by Eq.2.1. Results are presented for both perturbed and unperturbed dark energy. Note that the $\Delta\chi^2$ values given here are for the best fit points in the parameter space.

model. It is also bounded to give $-1 < w(z) < 0$ not to violate physical laws where it is in fact very difficult to explain theoretically any phenomena with $w(z) < -1$. Here z_t and the Δz are two parameters for the equation of state of dark energy. The first study set is carried out using 8 parameters amongst which six are the standard cosmological parameters and two are the equation of state parameters. We have considered a perturbed dark energy model for this case. Results are shown in Fig.9a and Fig.9b. The plot in Fig.9a shows that there is a negative correlation between the Hubble parameter and the z_t. Except that, the correlation between z_t and Δz with any other cosmological parameter is very weak. The likelihood surfaces of z_t and Δz are very flat, therefore the standard deviation in these parameters are very high. The estimated cosmological parameters are given in table 2. In Fig.10 we have plotted $H(z)$ and $Om(z)$ [15] [1] with their 95% confidence limits. We can see that decaying dark energy models can indeed have a consistent fit to the CMB data as well. Having z_t being allowed up to $z \approx 0.8$ is another interesting result that shows the big degeneracy present in the theoretical models fitting CMB data.

The second analysis is carried out using 5 parameters namely $\Omega_{0m} h^2$, h, A_s, z_t and Δz. We have considered a perturbed dark energy model for this case as well. Results are shown in Fig.11a and Fig.11b. The likelihood contours of z_t and Δz are very much flat and constraints on z_t and Δz are slightly tighter than the case of 8 parameter analysis. The estimated cosmological parameters are given in table 2.

It is worth mentioning that the best fit parameters for the ΛCDM model are $\Omega_b h^2 = 0.0224$, $\Omega_{0m} h^2 = 0.1336$, $h = 0.7097$, $\tau = 0.0848$, $n_s = 0.970$. The best fit parameters for the decaying dark energy model show an improvement of $\Delta\chi^2 = 1.3$ with respect to ΛCDM model. This improvement is not significant to consider this

[1] $Om(z)$ is given by $Om(z) = \frac{h(z)^2 - 1}{(1+z)^3 - 1}$.

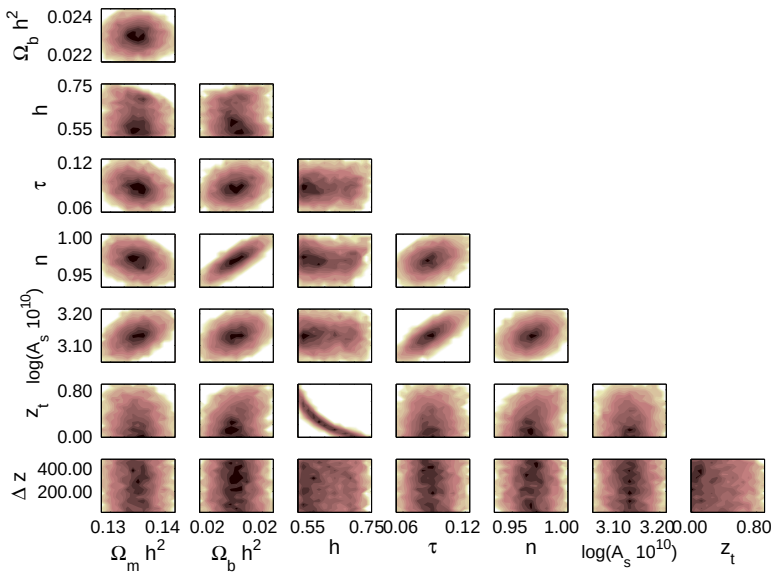

(a) Two dimensional likelihood contours for the set of 8 cosmological parameters

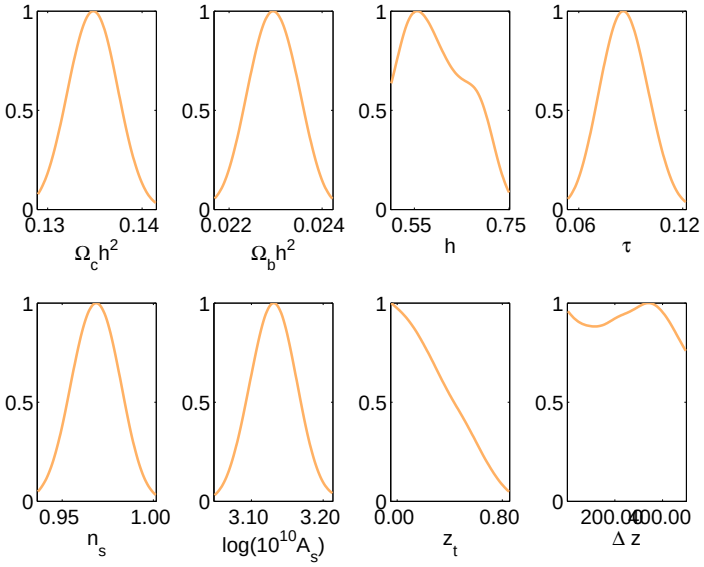

(b) One dimensional marginalized probability distribution

Figure 9: Cosmological parameter estimation (8 parameters) assuming perturbed decaying dark energy model. $H(z)$ for this model is derived by using the equation of state of dark energy given by Eq.3.1.

model being favored to the standard model but considering the fact that this model also has a better fit to the supernovae and BAO data in comparison to the the

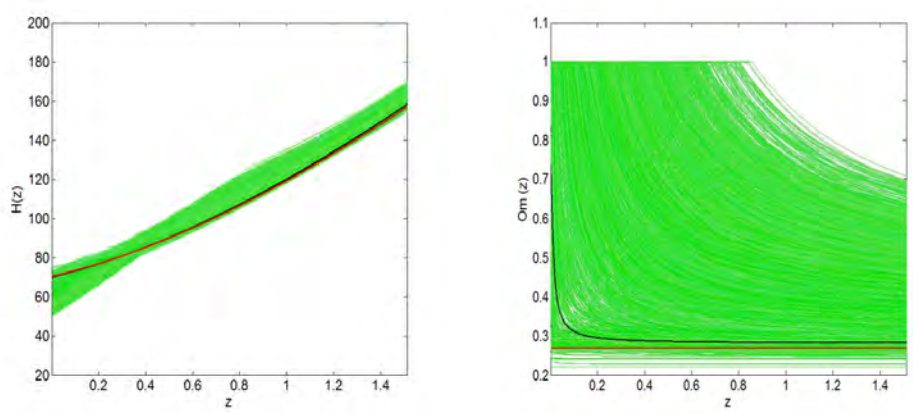

(a) (b)

Figure 10: 95% confidence limit of $H(z)$ and $Om(z)$ for the perturbed decaying dark energy model. $H(z)$ for this model is derived by using the equation of state of dark energy given by Eq.3.1. Black line is the best fit decaying dark energy model and the red line is the best fit ΛCDM model.

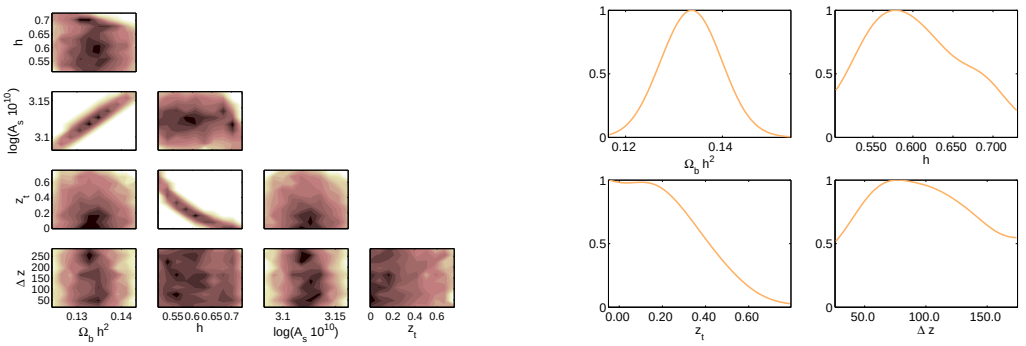

(a) Two dimensional likelihood for the set of 5 cosmological parameters

(b) One dimensional marginal probability distribution

Figure 11: Parameter estimation for the perturbed decaying dark energy model. $H(z)$ for this model is derived by using the equation of state of dark energy given by Eq.3.1 and other cosmological parameters are fixed at their best fit ΛCDM values.

standard model, this finding might be interesting. Looking at Fig.9b and Fig.10 we can see another interesting result that assuming a decaying dark energy model allows much lower values of H_0 to become consistent to the CMB data.

4. Conclusion

The analysis has been carried out by doing some analytical calculations estimating the effects of the changes in the expansion history of the Universe on the CMB angular power spectrum. Motivated by our analytical analysis we considered two different

	8 parameters		5 parameters	
	Average	Max-likelihood	Average	Max-likelihood
$\Omega_b h^2$	0.0224±0.0004	0.0224	0.0224	
$\Omega_{0m} h^2$	0.1343±0.0056	0.1357	0.1333±0.0048	0.1330
h	0.6929±0.032	0.6955	0.6974±0.0203	0.6995
τ	0.0865±0.0145	0.0849	0.0848	
n_s	0.9662±0.0129	0.9676	0.968	
$\log(10^{10} A_s)$	3.1295±0.0352	3.1340	3.1199±0.0153	3.1192
z_t	-0.7829±0.6768	0.0029	-0.4394±0.3081	-0.8008
Δz	270.71±138.6427	119.3598	142.8284±84.6293	144.3528
$\Delta\chi^2$		1.3		0.7

Table 2: Parameter estimation for the decaying dark energy model. $H(z)$ for this model is derived by using the equation of state of dark energy given by Eq.3.1.

forms of parametrizations for the expansion history and we studied the effect on the CMB low multipoles and ISW plateau using MCMC analysis. First parametric form assumes a Gaussian bump in addition to the $H(z)$ given by the standard ΛCDM model. Assuming this parametric form allow us to study how far we can deviate from ΛCDM model and still having a concordance to the data. This parametrisation also can help us to test the standard model itself and look for any possible deviation favoured by the data. Our analysis shows that it is possible to deviate up to 20% from the $H(z)$ given by the ΛCDM model at some intermediate redshift ranges and still having a proper fit to the data. Our analysis also shows that the spatially flat ΛCDM model is in proper concordance to the data and this model stands close to the centre of confidence contours. In the second parametric form we considered a decaying dark energy model at low redshifts. Our analytical and intuitive calculations indicates that increases in the expansion history at low redshifts might result to a better fit to the data. This is a feature of decaying dark energy models where we observe a slowing down of the acceleration in the expansion history of the universe. Indeed we realised that this parametric form can result to a better fit up to $\Delta\chi^2 = 1.3$ in comparison with the best fit ΛCDM model. This result indicate this slowing down model is not ruled out in favor of ΛCDM model by its CMB ISW effect. Considering the fact that these decaying dark energy models also are favoured mildly by supernovae and BAO observations, makes this finding interesting and worth further investigation. Another important outcome of our analysis, is that assuming different parametric forms of $H(z)$ results in significant changes in the posteriors of the cosmological parameters. For instance assuming the decaying dark energy model, H_0 can hold relatively smaller values than those expected from ΛCDM model and still having a good fit to the CMB data. This is another important issue in estimation of cosmological parameters using CMB data since it is also known that assuming different forms of the primordial spectrum affects significantly on the estimation of cosmological parameters [16]. The

recent results from Planck also suggest the deficit of power at low multipole ($\ell < 30$) is a feature of the CMB sky that may be worth addressing via ISW effect.

Acknowledgments

S.D. acknowledge the Council of Scientific and Industrial Research (CSIR), India for financial support through Senior Research fellowships. Computations were carried out at the HPC facilities at IUCAA. A.S. acknowledge the Max Planck Society (MPG), the Korea Ministry of Education, Science and Technology (MEST), Gyeongsangbuk-Do and Pohang City for the support of the Independent Junior Research Groups at the Asia Pacific Center for Theoretical Physics (APCTP). T.S. acknowledges Swarnajayanti fellowship grant of DST India.

References

[1] S. Das, Cosmic Microwave Background Anisotropy Numerical Simulation (CMBAns), Graduate school project report, IUCAA (2010)

[2] A. Shafieloo, V. Sahni & A. A. Starobinsky, Phys. Rev. D **82**, Rapid Communication, 101301 (2009)

[3] M. J. REES & D. W. SCIAMA, Nature **217**, 511 (1968)

[4] E. V. Linder, Phys. Rev. D **82**, 063514 (2010)

[5] E. V. Linder & T. L. Smith, JCAP **001**, 1104 (2011)

[6] J. Samsing, E. V. Linder & T. L. Smith, Phys. Rev. D **86**, 123504 (2012)

[7] http://camb.info A. Lewis & A. Challinor, Astrophys. J **538**, 473 (2000)

[8] E. Komatsu, et.al., Astrophys. J. Supl **192**, 18 (2011)

[9] A. Shafieloo, V. Sahni & A. A. Starobinsky, Annalen der Physik **19**, issue 3-5, 316 (2010)

[10] A. Shafieloo, V. Sahni & A. A. Starobinsky, AIPC **1241**, 294 (2010)

[11] Dodelson, S. Modern cosmology, Elsevier, (2003)

[12] P. Peebles, Principles of physical cosmology, Princeton University Press, Princeton, New Jersey, (1994)

[13] S. Hannestad, Phys. Rev. D **71**, 103519 (2005)

[14] J. Weller & A. Lewis, Mon.Not.Roy.Astron.Soc. **346** 987 (2003)

[15] V. Sahni, A. Shafieloo, A. A. Starobinsky, Phys. Rev. D **78** (2008)

[16] A. Shafieloo & T. Souradeep, New Journal of Physics **13**, Issue 10, 103024 (2011)

[17] WMAP likelihood software, http://lambda.gsfc.nasa.gov/product/map/current/likelihood_info.cfm